

LASER INTERFEROMETER GRAVITATIONAL WAVE OBSERVATORY  
- LIGO -  
CALIFORNIA INSTITUTE OF TECHNOLOGY  
MASSACHUSETTS INSTITUTE OF TECHNOLOGY

Document Type LIGO-T970218-02 - D Dec 1997

**Mode Cleaner Length/  
Frequency Control Design**

P Fritschel, N Mavalvala, D Ouimette

*Distribution of this draft:*

This is an internal working note  
of the LIGO Project.

**California Institute of Technology**  
**LIGO Project - MS 51-33**  
**Pasadena CA 91125**  
Phone (818) 395-2129  
Fax (818) 304-9834  
E-mail: info@ligo.caltech.edu

**Massachusetts Institute of Technology**  
**LIGO Project - MS 20B-145**  
**Cambridge, MA 01239**  
Phone (617) 253-4824  
Fax (617) 253-7014  
E-mail: info@ligo.mit.edu

WWW: <http://www.ligo.caltech.edu/>

LIGO DRAFT

# 1 BLOCK DIAGRAM OF SYSTEM

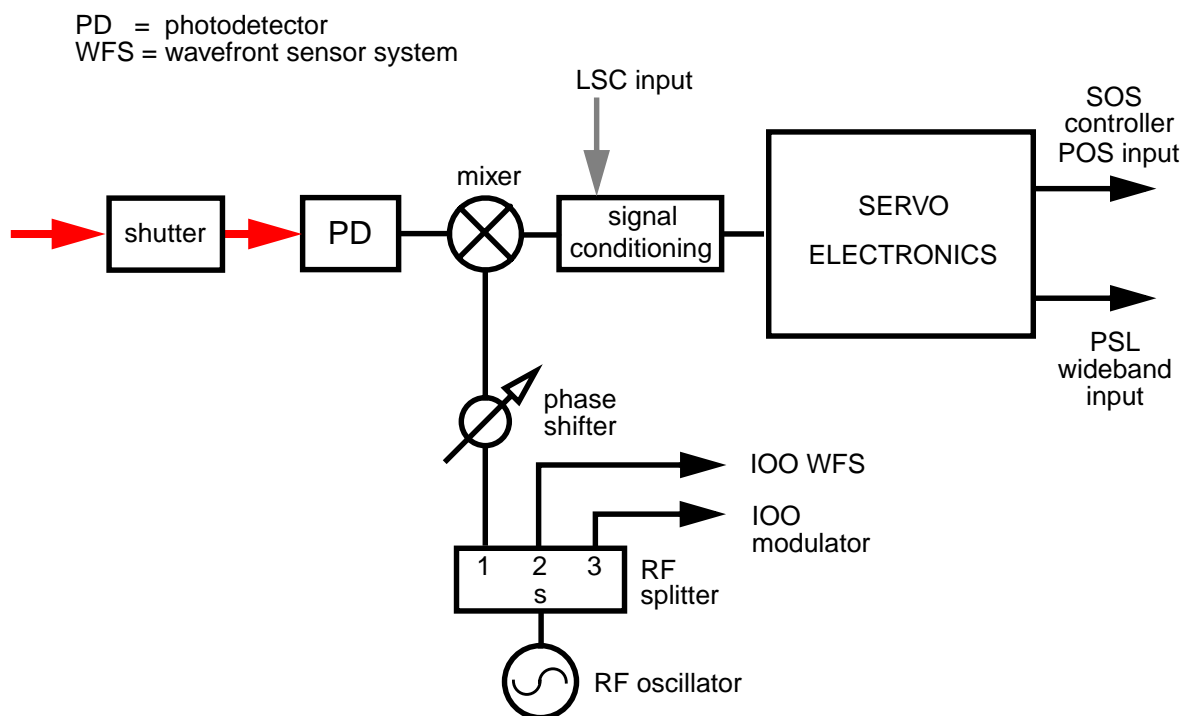


**Figure 1: Block diagram of the Mode Cleaner Length-Frequency control system.**

A block diagram of the length-laser frequency control system for the mode cleaner is shown in Figure 1. The servo control contains two paths – a fast path that corrects the laser frequency using the PSL wideband input, and a slow path that actuates on the mode cleaner length, through the POS/LSC input of the Small Optics Suspension (SOS) controller of one of the mode cleaner mirrors.

## 2 CONTROLS MODELING

### 2.1. Gain Requirements

The two functions of the mode cleaner servo are to keep the mode cleaner resonant with the input light and to suppress the frequency fluctuations of the input light to the required level. The

LIGO-DRAFT

required frequency suppression is determined by the allowed frequency noise on the light

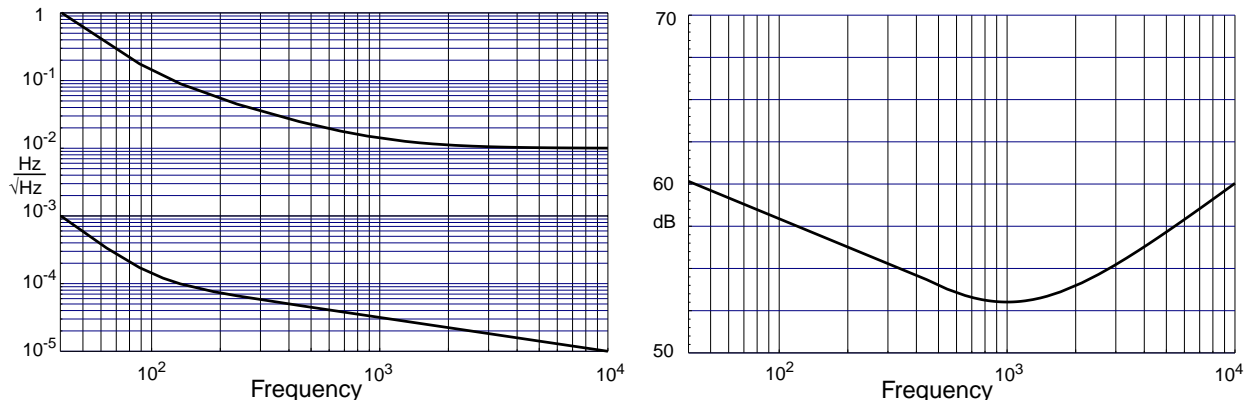


**Figure 2: Left graph: Frequency fluctuation requirements for the PSL (top curve) and IOO (bottom curve) subsystems (from SYS DRD). Right graph: Minimum frequency suppression factor (in dB) of the mode cleaner needed to suppress the PSL frequency noise to the required IOO level.**

delivered by the PSL subsystem, and the allowed frequency noise on the light delivered by the IOO. This is shown in Figure 2, along with the derived frequency suppression factor.

The other requirement is that the servo must have sufficient gain that the mode cleaner length deviates from the perfectly resonant length by no more than  $10^{-13} m_{\text{rms}}$ .

## 2.2. Servo Design

A block diagram of the servo is shown in Figure 3. The frequency of the laser light ( $F_{\text{PSL}}$ ) is compared with the resonant frequency of the mode cleaner ( $F_{\text{mc}}$ ) which is linearly related to the length of the mode cleaner, and converted into the demodulation voltage ( $V_d$ ) through the cavity pole filter ( $C_{\text{mc}}$ ) and the frequency-voltage converter ( $D_{\text{mc}}$ ). The demodulation voltage is pre-amplified and filtered ( $E_{\text{paf}}$ ), and further filtered in two paths: one that controls the laser frequency ( $E_l$ ); and one that controls the mode cleaner length ( $E_m$ ). These two signals are converted into frequencies by the PSL wideband actuator ( $H_l$ ), and the SOS controller ( $H_m$ ), acting on the mode cleaner length. The frequency of the light transmitted by the mode cleaner ( $F_{\text{transmitted}}$ ) consists of two components: the stabilized laser frequency low-pass-filtered by  $C_{\text{mc}}$ , and the resonant frequency of the mode cleaner high-pass-filtered by  $(1 - C_{\text{mc}})$ . The latter component is negligible in practice but is included in the diagram for completeness.

A detailed representation of the servo system blocks is shown in Figure 4. The preamplifier/filter,  $E_{\text{paf}}$ , consists of two filter stages in parallel. In acquisition mode a high gain bypass stage is disabled so that the overall loop gain rises as  $1/f$  down to 1 Hz (see Figure 5). In detection mode the bypass stage, which includes some aggressive filtering to achieve adequate frequency noise suppression at 7 kHz, is switched in. The laser path is AC coupled, so at low frequencies — typically below 2 Hz — the feedback is mainly to the mode cleaner length. This is necessary to ensure that the dynamic range of the VCO is not exceeded by frequency corrections due to seismic excitation of the mode cleaner length. A 40 dB stopband attenuation, 3 dB ripple elliptic

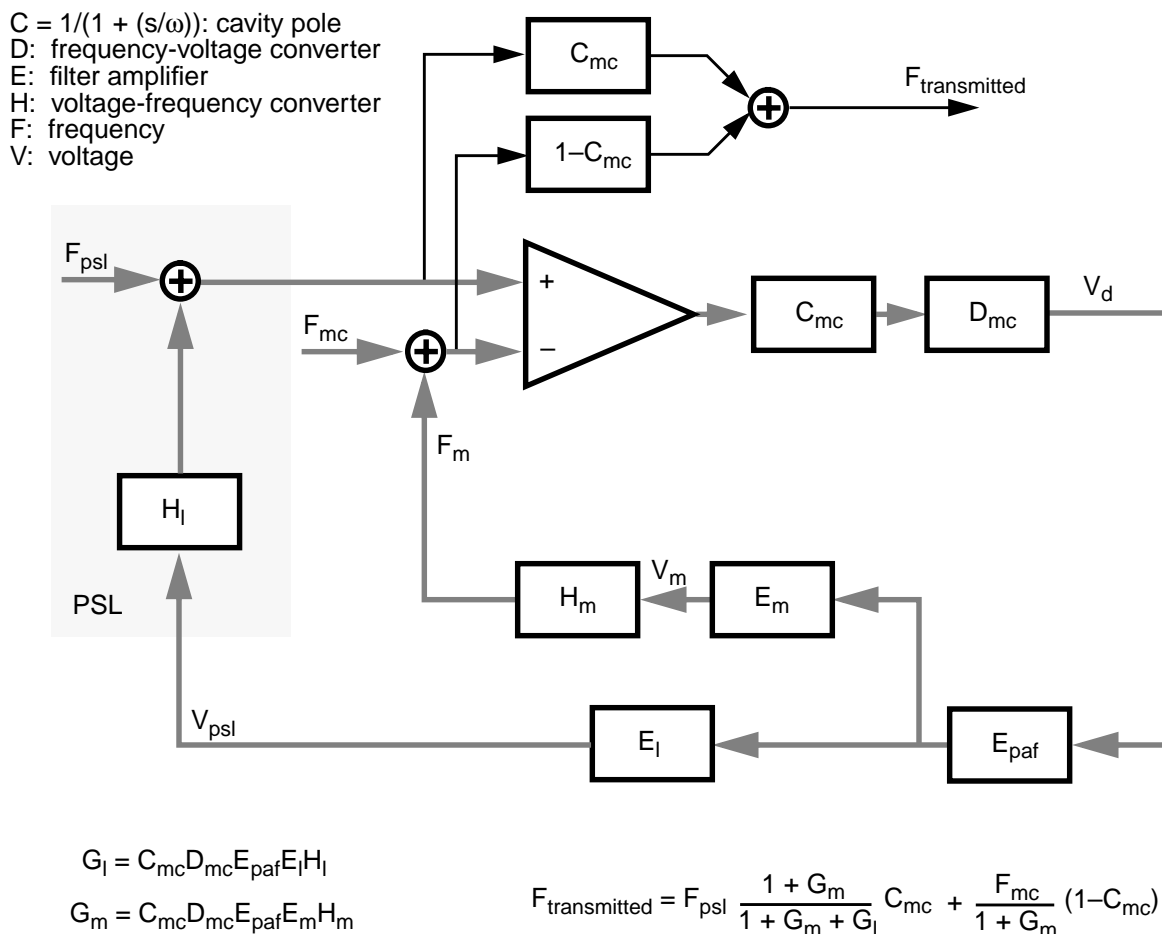


**Figure 3: Block diagram of the mode cleaner length/frequency servo. The loop gain expression at the bottom shows that the PSL laser frequency fluctuations are suppressed by the ratio of the total open loop gain to the gain in the mirror path (these expressions do not include the terms due to shot noise or electronics noise).**

filter at 30 Hz is included in the mode cleaner length path to steeply roll off feedback to the mode cleaner length by 40 Hz, where the relative gain between the length and frequency feedback must exceed 60 dB. At frequencies above a few hertz, the feedback is mainly to the wideband input of the PSL. The bandwidth of the loop is limited to 100 kHz by phase shifts due to transport delay in the acousto-optic crystal. This is simulated by the “VCO TF” block in Figure 4, which is merely a pole-zero pair at 300 kHz-3 MHz, producing 20° of phase lag at 100 kHz. To achieve 50 dB of gain at 7 kHz with a unity gain bandwidth of 100 kHz, a steep three pole filter at 300 Hz is rolled off with massive lead compensation at a few tens of kilohertz.

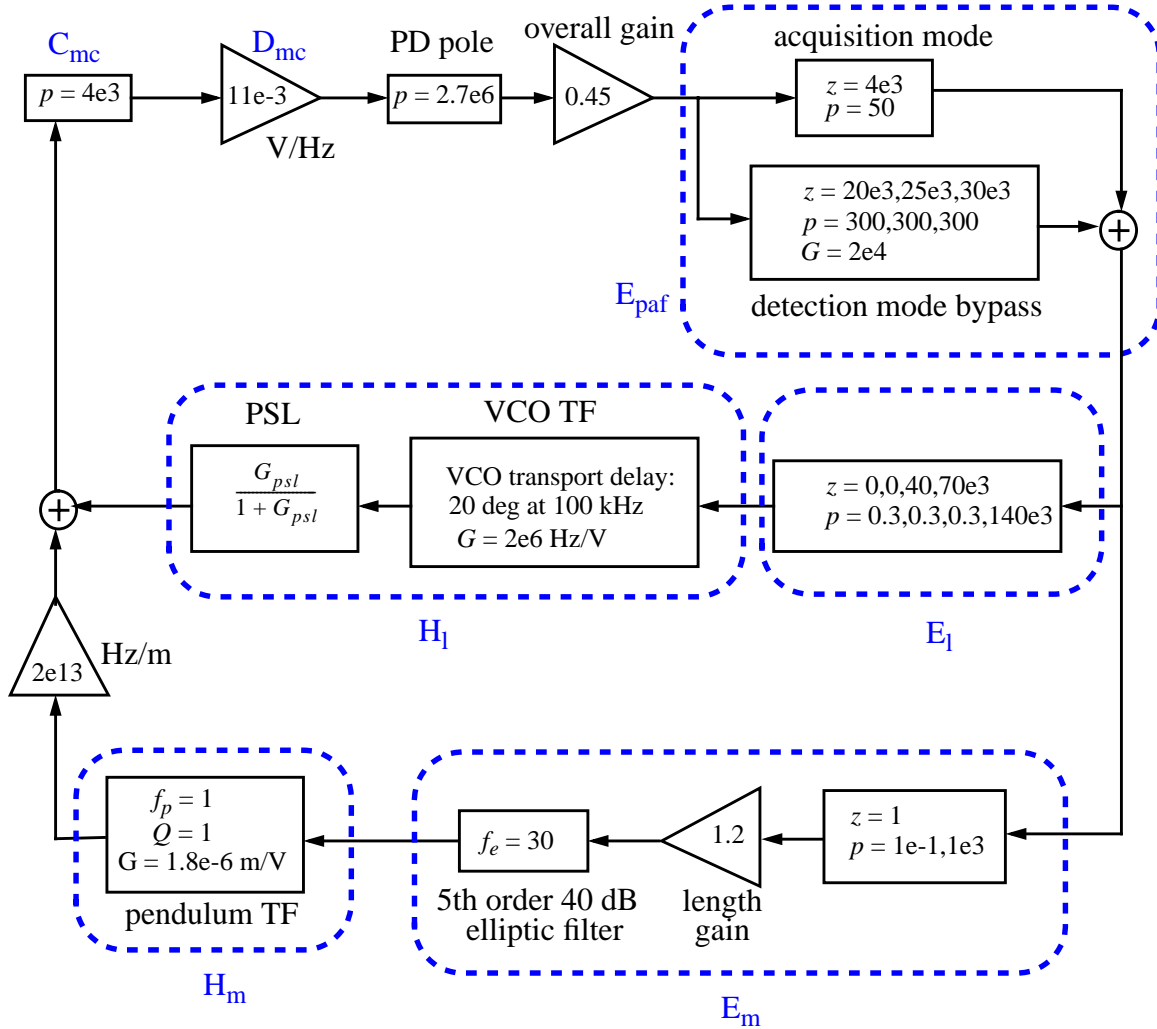
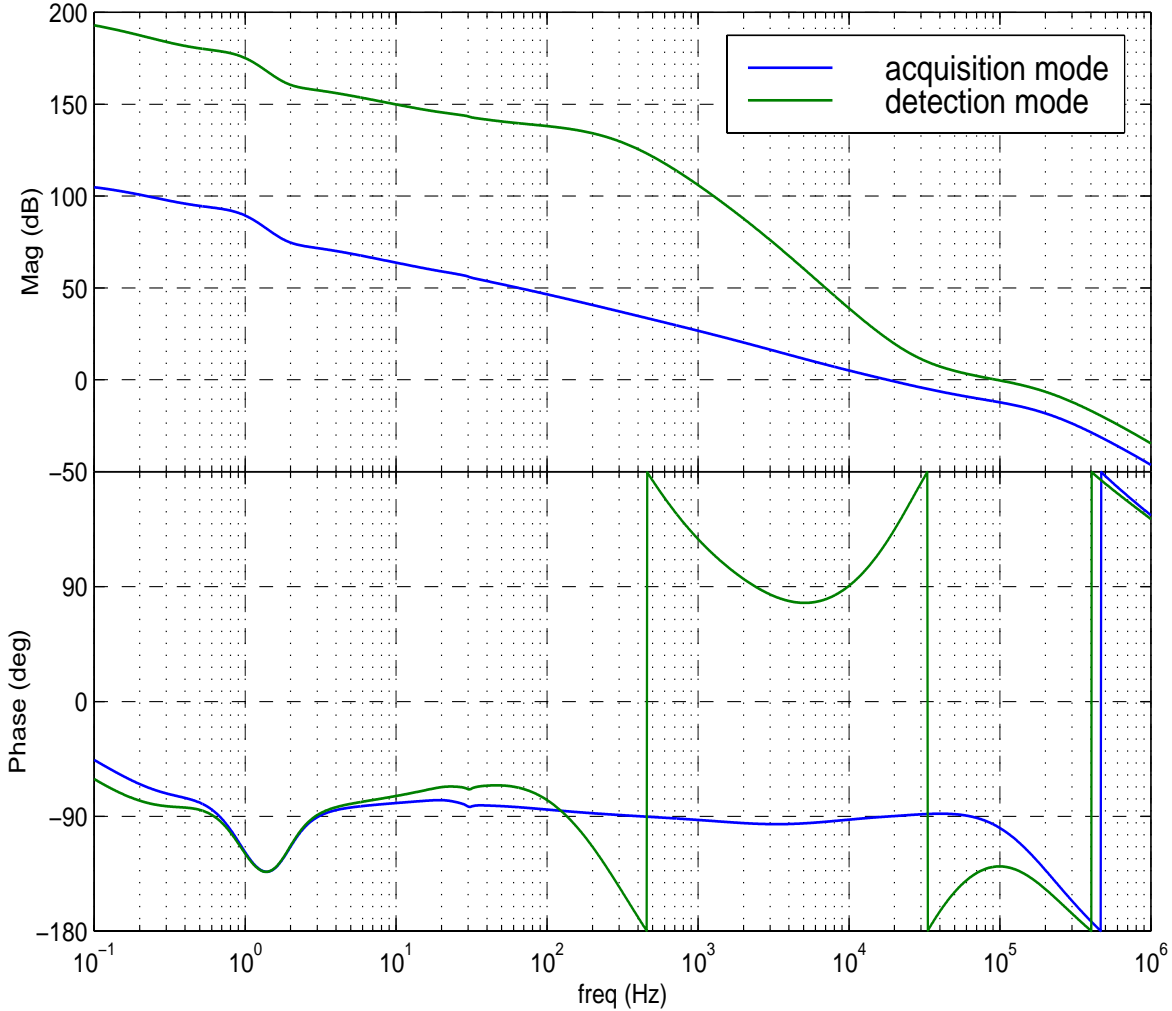


Figure 4: Control system blocks for the 2 km configuration.  $z$  refers to zero frequencies;  $p$  to pole frequencies;  $G$  to gain;  $f_p$  is the pendulum resonant frequency;  $f_e$  is the elliptic filter cutoff frequency. All frequencies are in Hz and gains are dimensionless, unless otherwise specified. For the 4 km configuration,  $C_{mc}$  is a pole at 3 kHz,  $D_{mc}$  is  $6.5e-3$  V/Hz and the PD pole occurs at 4 MHz. The loops are nearly identical, the only difference being that the overall gain for the 4 km configuration is 0.7.

### 2.3. Control System Performance

The control system shown in Figure 4 was implemented in a Simulink model to test the servo design. All model results shown in the figures are for the 2 km configuration. the 4 km configuration results are nearly identical. The control system performance for both configurations

is summarized in Table 1. In Figure 5, the open loop gains in both the acquisition and detection



**Figure 5: Open loop gains in acquisition mode (blue) and detection mode (green). Not included is the gain reduction by a factor of  $\sim 10$  during acquisition due to the lower transmission of the shutter in that mode. Thus (if not compensated for) the bandwidth for acquisition is about 2 kHz.**

modes are shown. In the acquisition mode the DC gain of the loop is 105 dB and the unity gain frequency is at 21 kHz. In the detection mode a high gain stage with additional filtering is switched in to meet noise requirements at all frequencies. In Figure 6 the detection mode loop gains for feedback to the mode cleaner length and to the laser frequency is shown. The feedback to the mode cleaner length crosses over with the laser feedback path at 2.0 Hz, with a relative phase of about  $100^\circ$ . This control design affords 50 dB of gain at 7 kHz, with a phase margin of  $50^\circ$  at unity gain bandwidth of about 100 kHz. The residual frequency noise at 7 kHz is  $1.7 \times 10^{-5} \text{ Hz}/\sqrt{\text{Hz}}$ , which just meets the frequency noise requirement at the output of the mode cleaner (see Figure 7). The loop gain limited residual length deviation is less than  $2 \times 10^{-17} \text{ m}_{\text{rms}}$  while a 1 mV electronic offset limits the residual length deviation to  $5 \times 10^{-15} \text{ m}_{\text{rms}}$ , which is

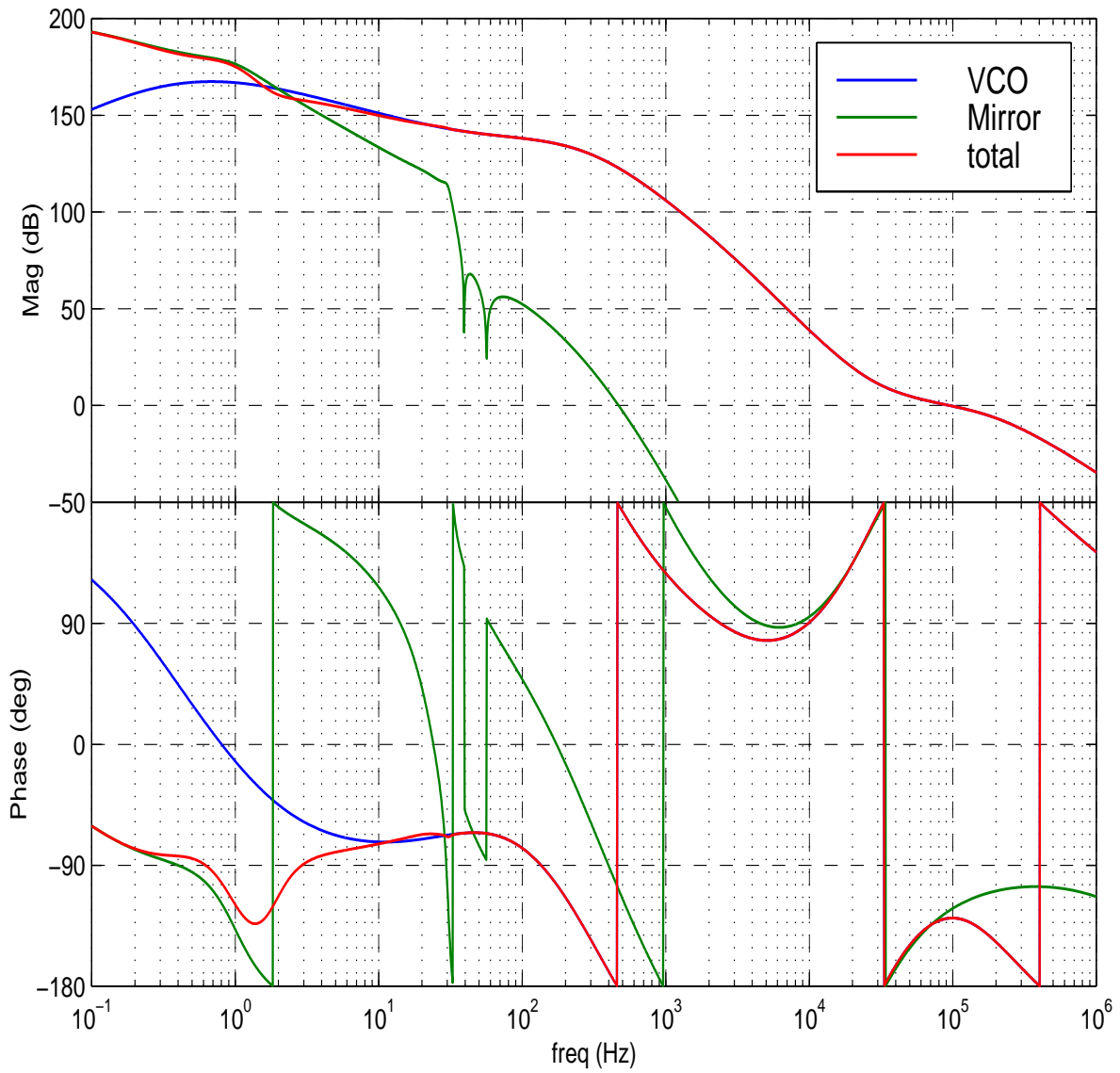


**Figure 6: Open loop gain (red curve) for the servo system with detection mode bypass stage engaged. Also show are the feedback to the mode cleaner length (green) and to the laser frequency (blue).**

LIGO-DRAFT

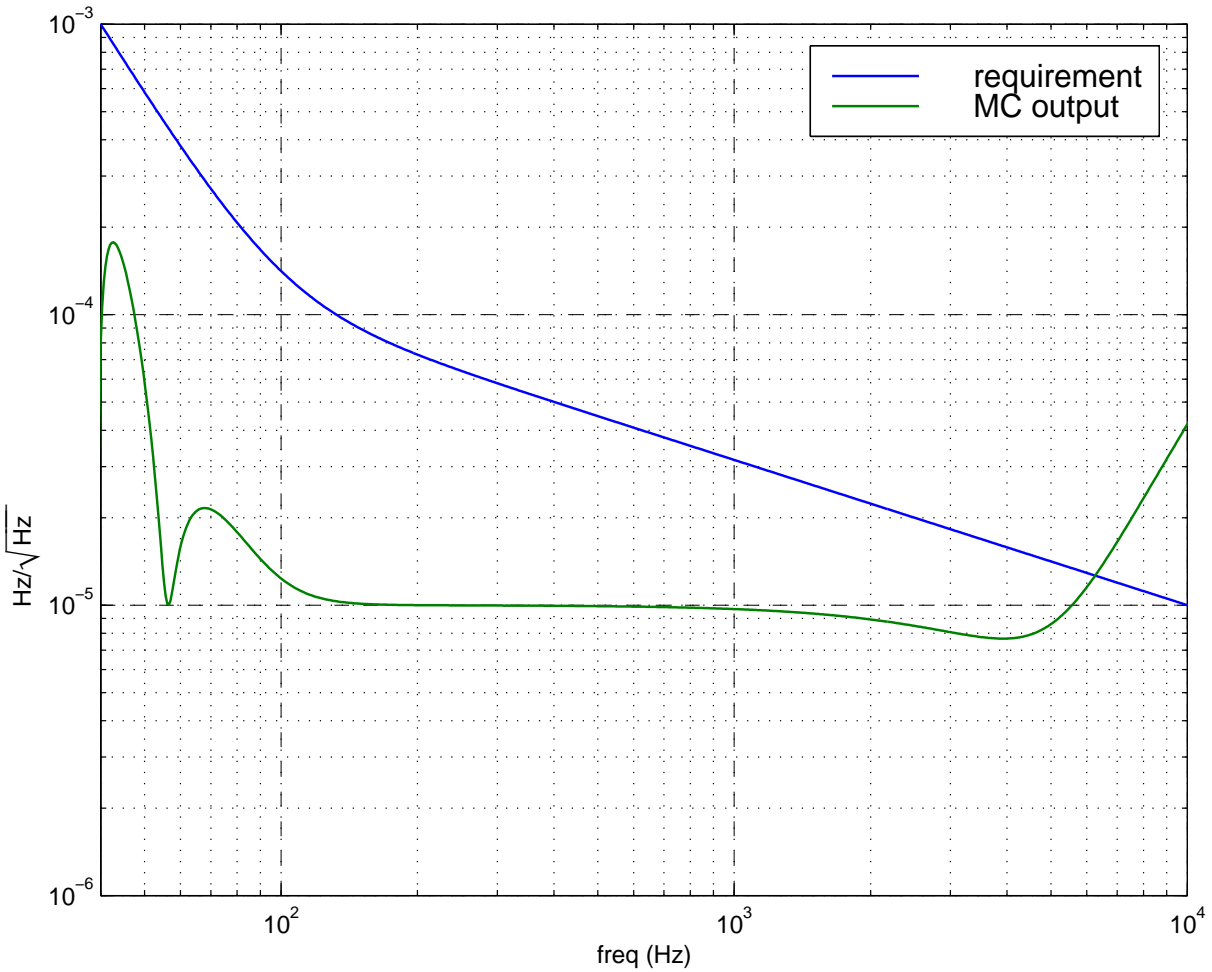


**Figure 7: Residual frequency noise at the output of the mode cleaner (limited by loop gain) compared with the frequency noise requirement. The requirement is specified out to 7 kHz only. Since the frequency noise requirement at the output of the mode cleaner is set by the thermal noise, if the residual frequency noise is limited by thermal noise rather than the loop gain, the residual frequency noise curve would coincide with the requirement.**

LIGO-DRAFT



well below the  $10^{-7} m_{\text{rms}}$  requirement. The spectral densities of signals at the wideband actuator input and the suspension coil driver input are shown in Figure 8. These correspond to  $0.05 V_{\text{rms}}$  at

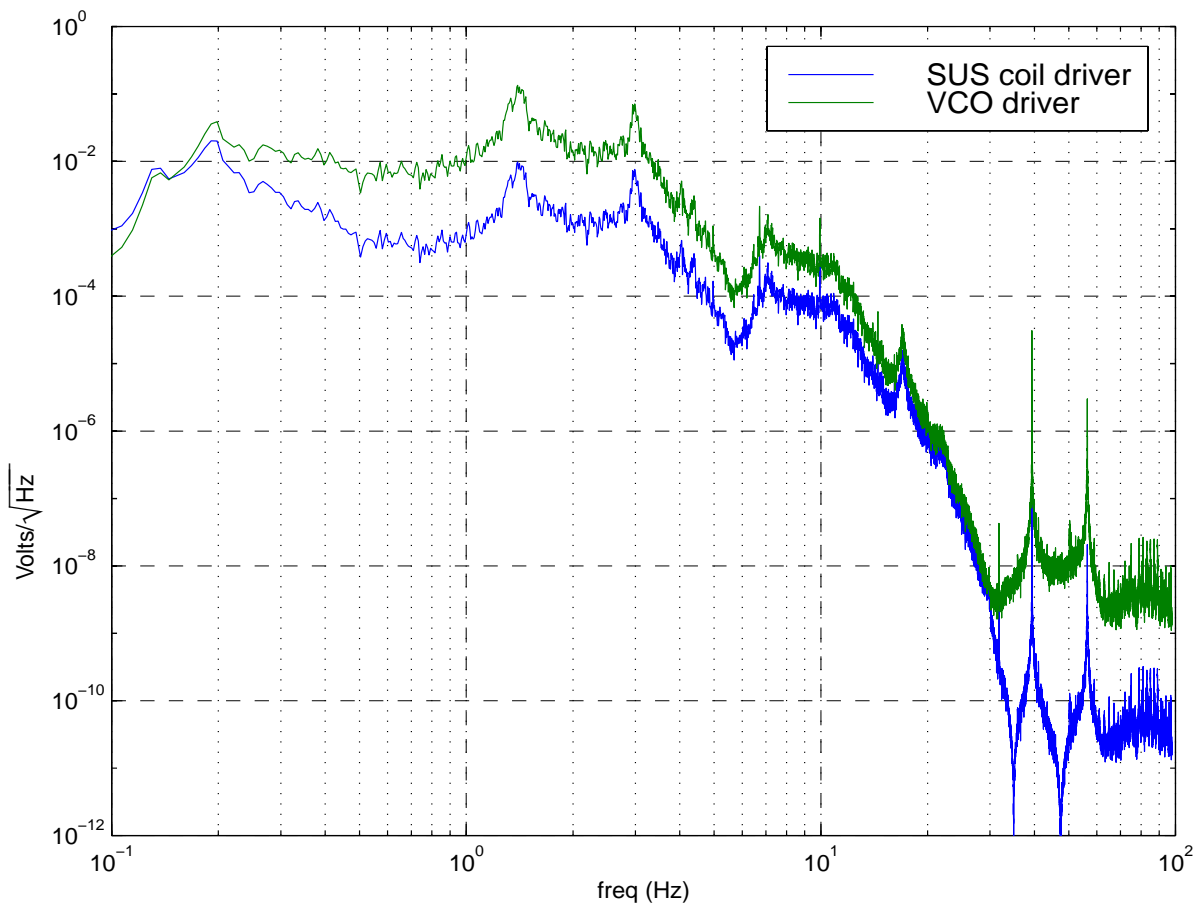


**Figure 8: Control signal inputs to the suspension coil driver (blue) and VCO (driver (green) with detection mode servo.**

the input to the VCO driver and  $0.006 V_{\text{rms}}$  at the coil driver input, respectively. Assuming that the peak-to-peak drive voltage at the VCO is a factor of  $30^1$  higher than the rms voltage, we get  $1.5 V_{\text{pk-pk}}$  at the VCO driver, which is 15% of the full dynamic range. This seems comfortably within the dynamic range of the VCO. We also note that in the band from 1 to 10 Hz the “noisy” Louisiana ground noise spectrum used as the seismic input to the model is uniformly a factor of 10 higher than the average ground noise we expect (as given by the so-called LIGO standard spectrum). It is, therefore, unlikely that the dynamic range of the VCO will be exceeded.

---

1. The peak-to-peak displacement is about a factor of 10 higher than the root-mean-square displacement. We use an additional factor of 3 as a safety margin.

A summary of the loop performance data for both the 2 km and the 4 km configurations are given in Table 1.

<i>Loop Data</i>	<i>Units</i>	<i>2 km</i>	<i>4 km</i>
Gain at DC	dB	190	190
Gain at 7 kHz	dB	50	50
Unity gain bandwidth	kHz	95	115
Phase margin	degrees	51	51
Length-frequency cross over frequency	Hz	2.0	2.0
<i>Performance Data</i>			
Residual frequency noise at 7 kHz	Hz/ $\sqrt{\text{Hz}}$	$1.7 \times 10^{-5}$	$1.5 \times 10^{-5}$
Residual length deviation			
Loop gain limited	$m_{\text{rms}}$	$1.8 \times 10^{-17}$	$1.9 \times 10^{-17}$
Electronic offset limited	$1 \text{ mV}_{\text{offset}} \Rightarrow 0.1 \text{ Hz} \Rightarrow 5 \times 10^{-15} \text{ m}$		
Control signal at VCO driver input	$V_{\text{rms}}$	0.054	0.054
Control signal at coil driver input	$V_{\text{rms}}$	0.0059	0.0059

**Table 1: Control system characteristics and performance data.**

## 3 ELECTRONICS DESIGN

### 3.1. Photodetection

#### 3.1.1. Optical Power level

The shot noise in the photodetection is the main factor in determining the fraction of the mode cleaner reflected power that is directed to the LSC photodetector; the shot noise must be small enough to not significantly limit the mode cleaner output frequency noise given in Figure 2. Frequency fluctuations incident on the mode cleaner are filtered by the low-pass  $C_{\text{mc}}$  (pole frequency of 4 kHz for the 4 km configuration), thus the ‘filtered sensing noise’ must be lower than the curve in Figure 2. This is most stringent at the high frequency limit of 10 kHz, where the frequency noise requirement is  $10^{-5} \text{ Hz}/\sqrt{\text{Hz}}$  and the filter attenuation is  $|C_{\text{mc}}| = 0.37$ . We thus choose to require a shot-noise level equivalent to  $10^{-5} \text{ Hz}/\sqrt{\text{Hz}}$  or smaller at 10 kHz, so that the shot-noise makes a negligible contribution (increase of 6% or smaller) to the transmitted

frequency fluctuations. The shot-noise limit at frequencies much below 4 kHz correspondingly must be  $3.7 \times 10^{-6} \text{ Hz}/\sqrt{\text{Hz}}$  or smaller; this level is given by:

$$\delta\tilde{\nu} = \left( \frac{c}{4p_{mc}F} \right) \sqrt{\frac{h\nu}{\eta P}} \frac{\sqrt{1 - J_0^2(\Gamma)MV}}{M J_0(\Gamma) J_1(\Gamma) (1 \pm \sqrt{1 - V^2})}$$

where  $p_{mc}$  is the round-trip path length in the mode cleaner,  $F$  is the finesse,  $M$  is the mode-matching coefficient,  $V$  is the cavity visibility,  $P$  is the total input power, and  $\eta$  is the quantum efficiency of the photodiode.

Table 2 gives the shot-noise frequency sensitivity for a range of values of mode-matching and visibility, scaled to an input power of 1 Watt. This shows that an effective input power of

sensitivity, $\times 10^{-5} \frac{\text{Hz}}{\sqrt{\text{Hz}}}$		Mode Matching, $M$			
		0.92	0.94	0.96	0.98
Visibility, $V$	0.95	1.09	0.99	0.88	0.77
	0.97	0.92	0.82	0.71	0.60
	0.99	0.74	0.65	0.54	0.42

**Table 2: Frequency noise sensitivity of the mode cleaner detection (for the 4 km IFO) as limited by shot-noise, for an effective input power of 1 W, a photodiode quantum efficiency of  $\eta = 80\%$ , and a modulation depth of  $\Gamma = 0.1$ .**

$P_{\text{eff}} = 1 \text{ W}$  is sufficient to meet the shot-noise sensitivity requirement. Since the power incident on the mode cleaner is 7.5 W (or slightly more), we need to detect  $\sim 13\%$  of the reflected light. The power incident on the photodetector when the mode cleaner is locked is roughly  $(2 - M - V)P_{\text{eff}}$ , and thus ranges from 30 – 130 mW for the above range of parameters. **A single 2mm diameter InGaAs photodiode will be sufficient for this application.**

### 3.1.2. Optical Gain

For a frequency change  $\delta\nu$ , the component of the optical power at the photodetector that oscillates at the modulation frequency is:

$$S_{\delta\nu} = \frac{8 J_0(\Gamma) J_1(\Gamma)}{\Delta\nu_c} \frac{\delta\nu(f)}{\sqrt{1 + (2f/\Delta\nu_c)^2}} P f_{\text{split}} \sin \omega_m t$$

where  $\Delta\nu_c = 8$  kHz is the linewidth of the cavity, and  $f_{\text{split}} = 15\%$  is the fraction of the input power ( $P$ ) that is detected. With a modulation depth of 0.1, the sensitivity  $D_v(f) \equiv S_{\delta v}/\delta v(f)$  at DC is  $D_v(0) = 5 \times 10^{-5}$  W/Hz.

Parameter	Value	
	4 km	2 km
Modulation frequency	33.3 MHz	26.7 MHz
Modulation depth	0.1	0.1
Optical frequency sensitivity,	$5.1 \times 10^{-5}$ W/Hz	$6.4 \times 10^{-5}$ W/Hz
Pole frequency	3.9 kHz	3.1 kHz
Photodiode capacitance, series resistance <sup>a</sup>	$C_d = 130$ pF, $R_s = 10$ $\Omega$	
Photodetector pole frequency	4.1 MHz	2.7 MHz
Photodetector transimpedance (resonant load $\times$ preamp gain $\times$ 0.5 for 50 $\Omega$ termination)	$150$ $\Omega \times 5 \times 0.5$	$200$ $\Omega \times 5 \times 0.5$
Voltage noise at PD output due to shot noise (assuming 30–130 mW on diode)	30–60 nV/ $\sqrt{\text{Hz}}$	42–84 nV/ $\sqrt{\text{Hz}}$
Frequency sensitivity @ mixer output (diode response: 0.7 A/W; mixer gain: 0.5)	6.5 mV/Hz	11 mV/Hz

**Table 3: Photodetection parameters for the mode cleaners of the 4 & 2 km IFOs. The preamp gains are scaled to produce the same frequency sensitivity at the mixer output (at DC) for the two cases.**

a. Diodes from several vendors are still under evaluation. The impedances of the diodes vary from vendor to vendor; values for the most likely case are given.

### 3.1.3. Photodetector

The photodetector will consist of a single photodetector module (single photodiode and preamp) of the type being developed for the LSC. This design will be documented separately once it is complete; some features of the design worth noting are:

- the load for the photocurrent is a tuned circuit made from the diode capacitance and a parallel inductor
- a trap for  $2f_m$  is included before the preamp
- the preamp is a low-noise wideband opamp, probably MAXIM 4106 or 4107, running at  $\pm 5$ V supplies; the voltage gain can be set ( $>5$  for the 4106,  $>10$  for the 4107)
- a low-pass filter, with a cut-off frequency above  $f_m$ , is included after the preamp to reduce high frequency noise into the mixer

- a readout of the DC photocurrent is included
- a monitor RF output is included (~20 dB lower than the main output)

The photodetector assembly will include an electrooptic shutter to control the light power on the diode before and during locking. The use of the shutter is described in section 3.4.

## 3.2. Demodulation & Signal conditioning

### 3.2.1. Mixer Level

During locked operation of the mode cleaner, the RF signal going into the mixer will be very small (10's of mV at most; see the results of the servo modeling). During lock, the mixer range should overly restrict the size of the demodulated signal. The photodetector preamp output can go up to ~3V-pk, or about 1.5V-pk at the mixer input, assuming a factor of 2 drop due to 50 ohm matching. This is equivalent to about 14 dBm of RF power. The mixer should thus allow a RF input level of up to 14 dBm. A Mini-Circuits, level 17S (such as the TAK-3H) is a good candidate.

### 3.2.2. Signal conditioning

Between the mixer output and the servo filtering stages, three signal conditioning functions must be provided:

- a low-pass filter immediately after the mixer, to filter out high-frequency noise (random & periodic) that can produce non-linearities in the amplifiers which follow
- a summing junction, to implement the 'additive offset' input for the LSC frequency control signal
- a variable-gain preamp, which allows adjustment of the overall loop gain

1. *Low pass filter.* The NPRO lasers are seen to contain noise peaks (AM & FM) in the 1–1.5 MHz region, which seem to come from the Lightwave Electronics NPRO controller. These noise peaks have been seen to produce broadband, audio-band noise in otherwise low-noise opamps, presumably through non-linear mechanisms. One solution is to passively filter out these peaks before the signal is amplified; in the PNI experiment, there is a 500 kHz 3-pole Butterworth low-pass which does an adequate job (note that these peaks are below the pole frequency of the pre-mode cleaner). The trade-off is the phase shift introduced by this filter, which can limit the servo bandwidth (which we would like to have not lower than 100 kHz). At the least, it is important to filter RF signals, from LO feedthrough or harmonics of the modulation frequency. If this is the only requirement, it could be met by using a ~5 MHz low-pass filter that would have no effect on the servo phase margin. The choice of filter type and cut-off frequency will be made as the servo modeling advances and we learn more about the noise of the 10 W laser.

2. *Summing junction.* The summing junction for the additive offset input will be included immediately after the low-pass filter, before the preamp, so that the sensitivity of this input (Hz/V) is independent of the preamp gain (for frequencies where the mode cleaner loop gain is reasonably high). The additive offset input will be summed with a gain of unity relative to the low-pass filter output. When the MC is locked, the signal at this input is compensated by a signal

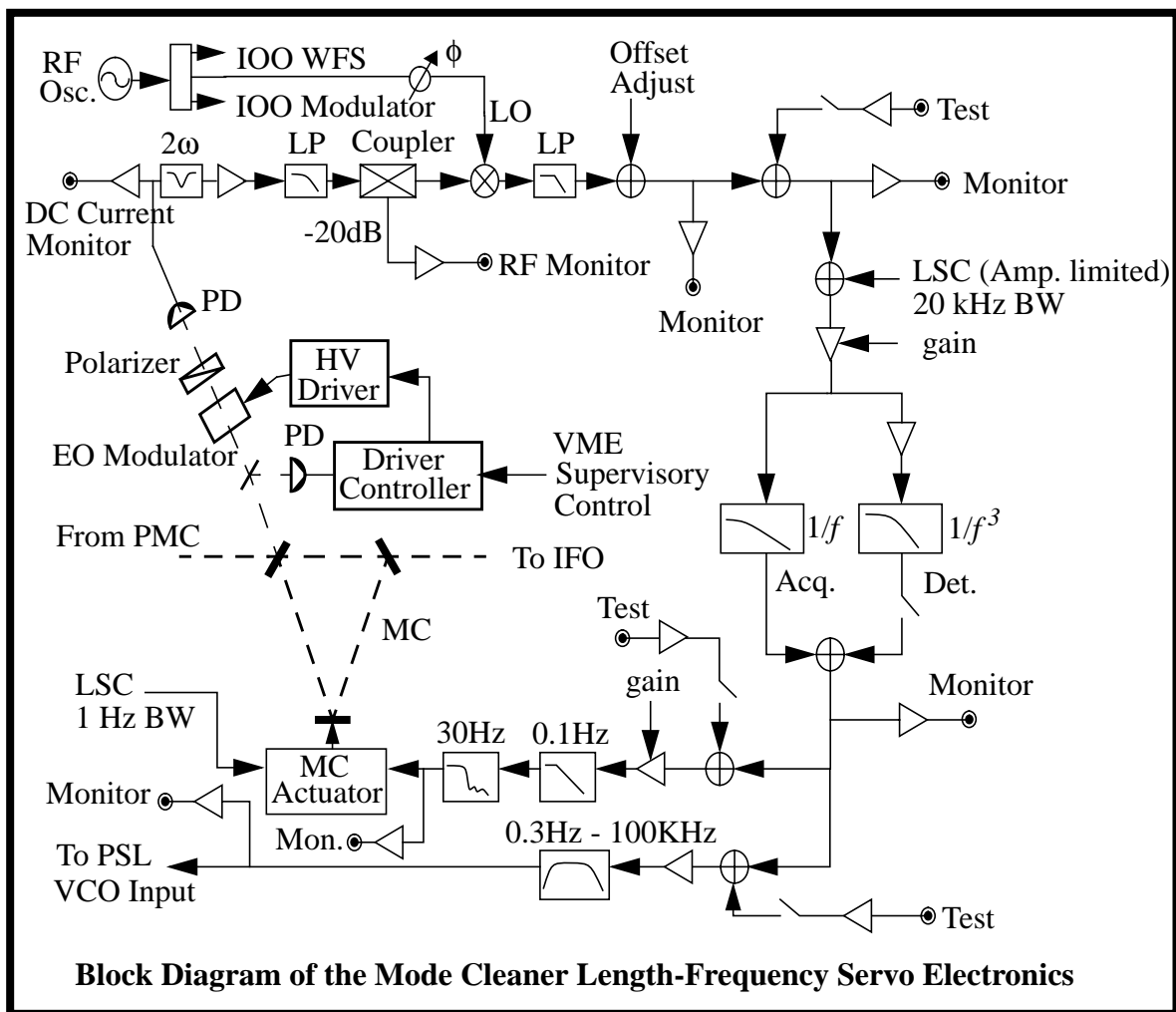
of nearly equal magnitude and opposite sign from the mixer (low-pass filter) output. Since the maximum mixer output is  $\sim 1\text{V-pk}$ , this gives a frequency tuning range for the AO input of  $\sim 100\text{ Hz}$ . The AO input will include some form of voltage limiting at a level TBD ( $\sim 1\text{V}$ ), to prevent injected signals from throwing the MC out of lock.

3. *Preamplifier*. The requirements of the variable-gain preamplifier are:

- input voltage noise less than  $7\text{ nV}/\sqrt{\text{Hz}}$  above  $40\text{ Hz}$  (so that it is at least  $20\text{dB}$  lower than shot noise in all cases)
- gain control: Range: at least  $\pm 15\text{dB}$  about nominal gain level; Resolution: no coarser than  $1\text{ dB}$  steps; Nominal gain: TBD ( $\sim 10\text{ dB}$ )
- bandwidth:  $> 1\text{ MHz}$  at all gain settings (less than  $5^\circ$  phase lag at  $100\text{ kHz}$ )

### 3.3. Servo electronics

#### 3.3.1. Block diagram



### 3.3.2. Noise & Range requirements

*TBD.*

### 3.3.3. Gain control

Overall gain control, which determines the bandwidth of the loop, is afforded by the preamplifier gain control described in section 3.2. Additional gain control will be provided in the mode cleaner length (mirror) servo path. This gain control will serve to determine the crossover frequency between the two paths, without affecting the overall bandwidth. Specifications for this gain control are:

- Range: at least  $\pm 15$ dB about nominal gain level
- Resolution: no coarser than 1 dB steps

### 3.3.4. Test & Monitor points

For measuring the closed loop response of the system, test inputs and outputs will be provided as follows:

- Global unity gain test input-output, shortly after the mixer (before, after, or incorporated into the preamplifier); this is used to measure the overall gain
- Test input at the input to the length/mirror path of the servo, used to measure the gain in this path
- Test input at the input to the laser/VCO path of the servo, used to measure the gain in this path
- Test output at the point where the servo splits between the length and laser paths; used in conjunction with the above two inputs to determine the gain in the separate paths

The following points in the servo will have buffered monitor outputs:

- Mixer/LPF output
- Control signal sent to the PSL/VCO
- Control signal sent to the SOS controller input

## 3.4. Lock Acquisition

### 3.4.1. Electro-optic Shutter

Before the mode cleaner is locked, the full incident power (7.5 W) is reflected. Approximately 15% of the reflected light is detected by the length detector when the MC is locked, thus there would be  $\sim 1$  W of light on the detector when unlocked. This is too much power for the diode. The power incident on length detectors (and WFS) will be controlled by a variable attenuator consisting of an electro-optic modulator and a polarizer. Such an attenuator will provide fast shut-off when the MC loses lock, and selectable intermediate transmission states. A schematic is shown in Figure 9. A fast photodetector ( $PD_A$ ) sampling a fraction of the light incident on the attenuator provides a trigger/reference level. When the MC is unlocked, a high level on  $PD_A$  keeps the attenuation factor at a high value (10-100 $\times$ ) so that the power incident on the length

sensor is below  $\sim 100$  mW, but still large enough to allow locking of the MC. Once the MC is locked, as indicated by the level of  $PD_A$ , the attenuator is opened up to a transmission of  $\sim 100\%$ . A flow diagram for the shutter operation is shown in Figure 10.

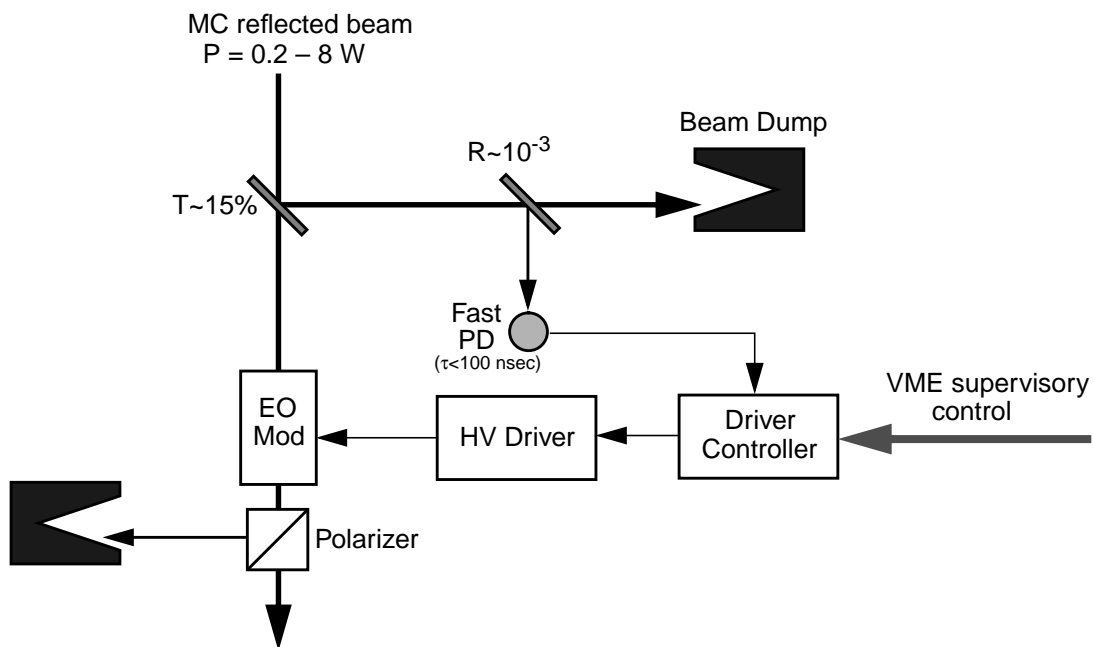


**Figure 9: Schematic of the EO shutter, auxiliary optics, and drive electronics.**

<i>Function</i>	<i>Options</i>
Shutter closed level select	T = -10, -15, -20 dB
Shutter open level select	T = 0, -3, -6 dB
Activate automatic open	Yes/No
Lock trigger level select	$\pm 20$ dB about nominal TBD level, in steps of 3-4 dB

**Table 4: Supervisory controls available for the Driver Controller.**

LIGO-DRAFT



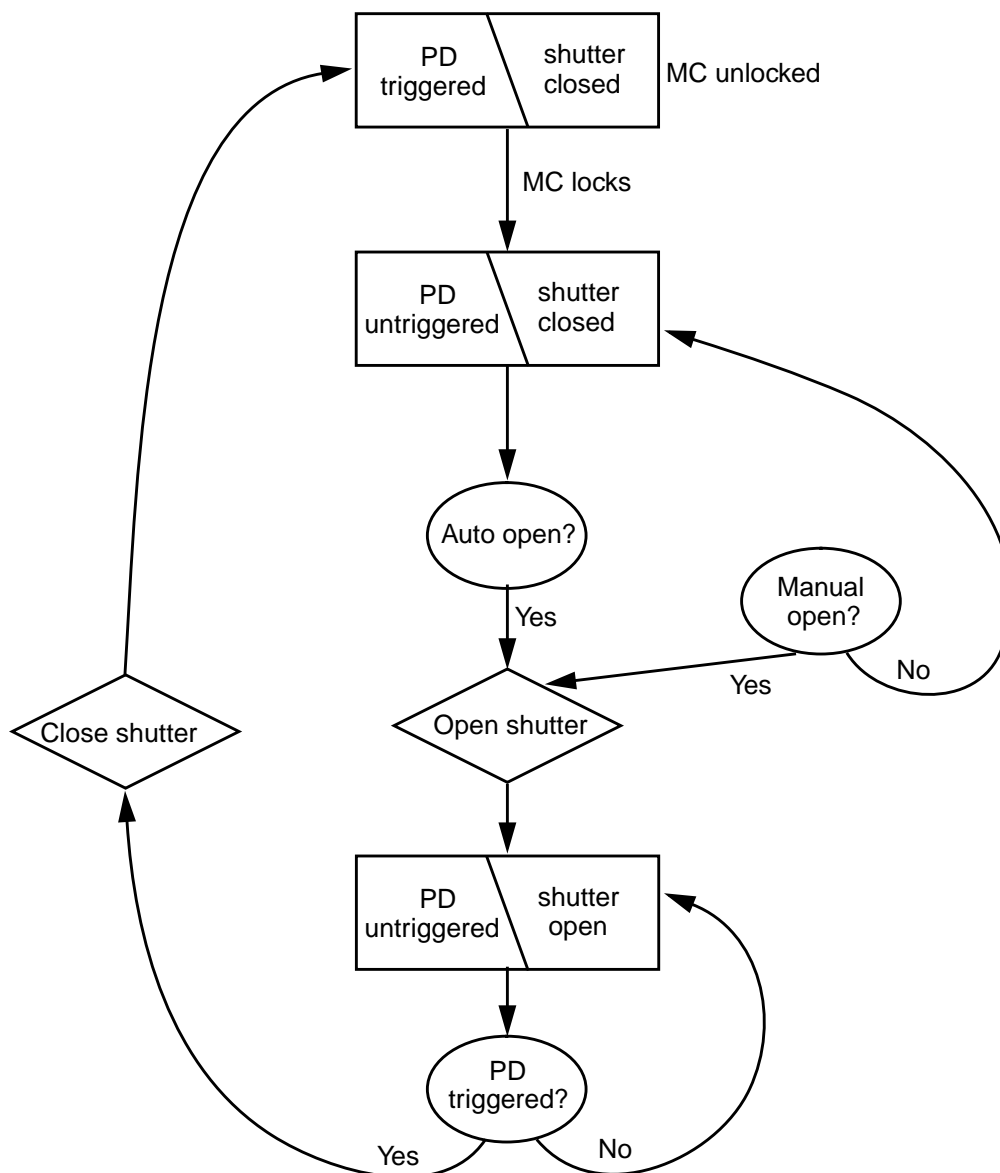


**Figure 10: Flow diagram representing the operation of the shutter.**

### 3.4.2. Acquisition Servo

Since the operational servo is not stable over the factor of  $\sim 10$  range of optical gain that occurs when the shutter switches state, a separate acquisition mode servo state is required. This servo state is also useful for operating the mode cleaner in the presence of large modulations of the input beam power. The loop response in this mode will have a simple  $1/f$  response above  $\sim 1$  Hz. As shown in section 2, the acquisition mode merely switches out a bypass gain stage between the mixer and the laser-length split.

A visibility monitor function will serve to indicate the lock status. This will also trigger the transition from the acquisition servo to the higher-gain operational servo (when in automatic mode for the bypass gain stage control).

## 4 USER INTERFACE & DIAGNOSTICS

There will be a combined control/diagnostic operator's screen for the length/frequency and alignment control of the mode cleaner. Here we outline the features that will be included for the length/frequency portion.

### 4.1. Status Information

The status information listed in Table 5 will be graphically displayed on the mode cleaner operator screen.

<i>Status</i>	<i>Description</i>
Lock Status	Color indicator (e.g.: green: locked and running; yellow: acquiring lock;
Gain state	Indication of acquisition or detection mode gain
Shutter activation	Indication of automatic or manual shutter control.

**Table 5: Status information to be displayed on the control screen.**

LIGO-DRAFT

## 4.2. User controls

User controls for the mode cleaner servo are listed in Table 6; other user controls for the shutter driver were given in Table 4 above.

<i>Control function</i>	<i>Description</i>
Bypass Stage control	Controls activation of the bypass gain stage. Three options: <b>Off</b> (not connected); <b>On</b> (manual switch-in of bypass); <b>Automatic</b> (bypass switches in automatically upon lock acquisition)
Preamplifier gain control	Selection of the preamplifier gain, as described above
Length path gain control	Selection of gain in the length (mirror) servo path, as described above
Demodulation phase	Phase shifter adjustment for LO. 360 deg. range; < 5° resolution.
Modulation amplitude	Amplitude control for the RF modulation. Modulation depth range: 0-0.2 rad-pk; steps of 0.01. (Requires 50 mW max RF power if NewFocus modulator is used.)
Offset control	Selection of offset added to mixer output. Can be used to zero mixer offset, or for diagnostic purposes. Range: $\pm 1\text{V}$ ; resolution: $1\text{V}/2^{15} = 30\ \mu\text{V}$ .

**Table 6: User control functions to be implemented on the operator screen.**

LIGO-DRAFT

### 4.3. Signal Monitoring

The signals listed in Table 7 will be displayed on the mode cleaner operator screen.

<i>Monitor</i>	<i>Description</i>
Input light level	DC photodiode on PSL/IOO table. Digital voltage readout, with calibration in watts.
Output light level	PSL intensity stabilization photodiode, calibrated in watts.
Laser Control signal	MC control signal sent to PSL (VCO driver). Digital readout, with range indication.
Length Control signal	MC control signal sent to the SOS coil driver. Digital readout, with range indication.
Visibility monitor	Cavity visibility function, made using input light level PD and DC output of MC RF PD. Digital readout plus meter.
Demodulator output	Mixer output monitor, taken after the offset adjustment.
LO level	Indication of the RF level at the LO input. Digital readout.
Shutter Fast PD level	Light level on the shutter triggering PD. Digital readout.
EO Driver level	Voltage level applied to the EO modulator. Digital readout.
RF PD temperature	Readout of temperature sensor on RF photodiode.
Video camera image-1	Image from camera looking at a sample of the MC transmitted beam, to check mode.
Video camera image-2	Image from camera looking at a sample of the MC reflected beam.

**Table 7: Monitor signals to be displayed on operator screen.**

LIGO-DRAFT

#### 4.4. Diagnostics functions

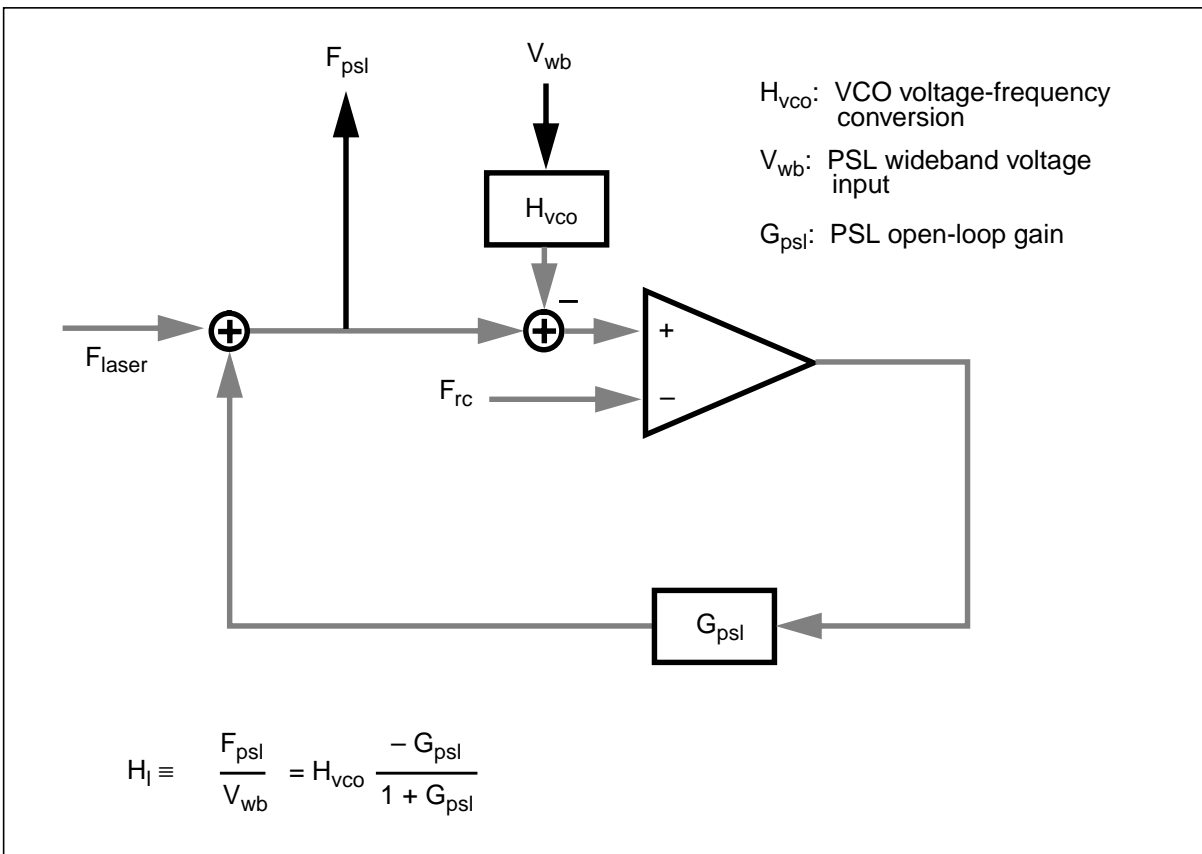
The mode cleaner length/frequency control system will rely on the following capabilities to perform self-diagnostics that may be initiated from the operator console.

<i>Function</i>	<i>Description</i>
Ringdown Measurement	If the capability exists to turn off the laser quickly, a ringdown measurement will be implemented, using the PSL power stabilization photodetector.
Loop Gain Measurement	The capability of making a single frequency closed loop gain measurement will be incorporated into the system, using the global test input-output. Selection of frequency TBD.
Lock Offset Measurement	Measures coupling of amplitude modulation on the input light (PSL function) to the MC error signal, to infer offset. May just be part of a global AM coupling test.

**Table 8: Diagnostic functions to be performed from operator screen.**

LIGO-DRAFT

## APPENDIX 1 PSL VOLTAGE-FREQUENCY CONVERSION



## APPENDIX 2 DAQ CHANNELS

From the MC Length/Frequency control system, the signals listed in Table 9 will be acquired by the CDS DAQ system.

**Table 9: Signals from the MC Length/Frequency control system that are acquired by the DAQ.**

Name	ID	Bits	Rate	Description
MODECLEANER_I	5000	16	16384	mode cleaner length sensor, I-phase
MODECLEANER_Q	5001	16	16384	mode cleaner length sensor, Q-phase
LENGTH_MC	5002	16	512	control signal for mode cleaner length
LASER_FREQ_MC	5003	16	16384	control signal for laser frequency